On-chip Magnetoresistive Sensors for Detection and Localization of Paramagnetic Particles

Samyak Shah and Hadi Heidari
Magnetoelectronics Lab (meLAB), School of Engineering, University of Glasgow, G12 8QQ, UK
Hadi.Heidari@glasgow.ac.uk

***Abstract*— This paper presents the work towards miniaturized magnetic biosensor array based on the detection of paramagnetic particles using the giant magnetoresistance (GMR) effect. GMR sensors have been studied for many years, but its application for on-chip integration and in complex configurations, as well as effective localization for Lab-On-Chip and Tissue Engineering applications is not yet explored. This work demonstrates the development of initial prototypes of 5 and 9 sensor GMR arrays of varying geometries and corresponding calibration and localization algorithms to detect and localize paramagnetic materials in 2D. The generation of a uniform magnetic field using a 16 magnet Halbach cylinder was also analyzed and optimized using FEA for different sensor configurations. Results show excellent localization for the fully calibrated 5 sensor arrays, with a mean (SD) error of 2.45 (1.61) mm for the ferrofluid as compared to 1.48 (1.14) mm for a strong ferromagnet for a 25×25mm^2 array surface. The 9-sensor array similarly showed good results for full calibration.**

Keywords — Giant Magnetoresistive (GMR); Lab-on-Chip; Detection; Localization; Paramagnetic Particles.

I. INTRODUCTION

Magnetic biosensors are analytical micro-devices with biological high-sensitivity elements, integrated in physicochemical sensors and retaining a magnetic field. Due to their low background noise and high long-term stability [1,2], magnetic sensing technologies have become increasingly useful for biomedical field, particularly in Lab-On-Chip applications [3]. Due to the advances in magnetic and nanofabrication technologies, sensors are becoming both smaller and more sensitive, leading to the development and use of magnetic sensor arrays [4,5]. These advances have allowed the integration and multiplexing of Hall and GMR sensors onto sub-1mm^2 CMOS chips [1,6,7,8,9]. These arrays have been used for research by both military and academia [4], and can differentiate between individual particles. Most biosensors are currently made on a rigid substrate, though future sensing systems will also require flexible arrays.

Whilst magnetic sensors arrays were initially only considered for biosensing, consideration is now also being given to other applications. The sensor arrays can be coupled together with a method of magnetic manipulation, and subsequently the system can be used for cell sorting and patterning applications [5]. Such a system was created using a TMR magnetic sensor array, and conducting line patterns that had the potential to move single magnetic microbeads. Recent reports have also outlined the potential of magnetic sensors and sensor arrays in tissue engineering, especially in 3D tissue fabrication where an array can be used as a method to sense

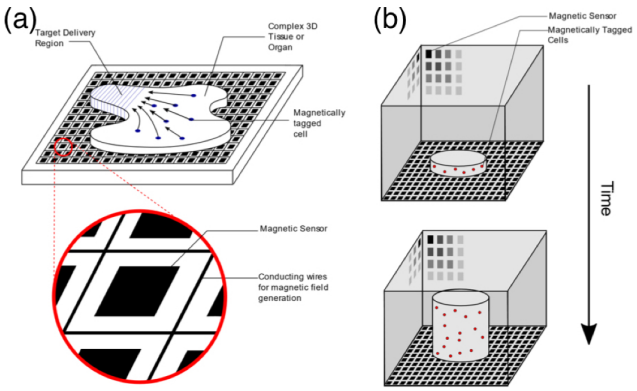

Fig. 1. (a) Application of sensor array and conducting wires to deliver cells to a particular region of a complex tissue or organ. **(b)** Application using localization of particles to monitor growth of 3D tissue [10].

fiber alignment and orientation in real-time [10,11]. This has already been shown to be theoretically feasible using a GMR sensor array [11].

This paper serves as a proof of concept for the creation of the underlying GMR based magnetic sensor array system and algorithm that can localize a paramagnetic material in 2D space.

II. DETECTION OF MAGNETIC PARTICLES

The typical working principle of magnetoresistive sensors for biological/chemical targets detection is based on the immobilization and subsequent detection of bioanalyte/magnetic nano-particle conjugates on the surface of the sensor device. The immobilization of magnetic particles on the sensor device commonly uses biomolecular interactions, e.g., antigen-antibody, and thus requires functionalization via biological/chemical treatment [6].

Detection will occur through sensing of the magnetic field. The GMR effect demonstrates large changes of resistance in the presence of an applied magnetic field, making it well suited for detection of minute magnetic fields, as explained in Fig. 2. Assuming antiparallel Ferromagnetic (FM)-Nonmagnetic (NM) multilayer coupling, the first magnetic layer will act as a spin-polarizer for inbound electrons. When multilayer is not in the presence of a magnetic field, a scattering of polarized electrons will occur, leading to a large resistance. In presence of an applied magnetic field, a parallel arrangement will result. The electrons will not be scattered, increasing their mean free path and reducing resistance.

The magnitude of the effect is mainly dependent on the materials used in the multilayer, with resistance changes of

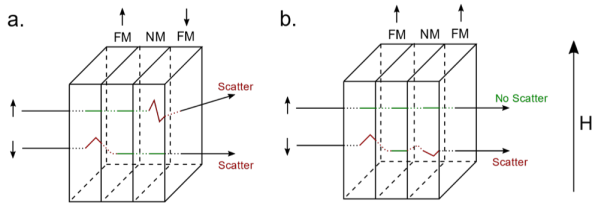

Fig. 2. GMR antiparallel multilayer in (a) the absence, and in (b) the presence of magnetic field H.

120% and 220% being reported for Co/Cu and multilayers [12]. However typically the range is 10-20% at room temperature. Though there are other magnetic sensing technologies available such as OMR/AMR and Hall Effect sensing, GMR is used here as it is the most sensitive and stable current commercially available technology. Tunneling Magnetoresistance (TMR) is a promising future technology for this application, providing an average change in resistance of 70% at room temperature, but they are still challenging to manufacture [12].

III. Localization Algorithm

The algorithm designed to localize the position of the magnetic particle is a weighted average, as shown by equations (1) and (2). This method of localization will increase the resolution of the system by being able to localize particles in between n sensors. The center of the array is taken to be (0,0).

$$x_{wa} = \sum_1^n \frac{val_i}{maxval_i - minval_i} \cdot x_i \qquad (1)$$

$$y_{wa} = \sum_1^n \frac{val_i}{maxval_i - minval_i} \cdot y_i \qquad (2)$$

Due to imperfections in hand-soldering and in the uniform perpendicular magnetic field, all the sensors need to be calibrated so that a maximum value can be established for the weighted average. In the future, machine soldering and a more uniform magnetic field can be used to prevent this issue. This algorithm was coded into processing along with the calibration algorithm, which would record the maximum and minimum values of each sensor.

IV. Expriments and Discussion

This work is a step towards on-chip magnetic manipulation and localization. In this regard, GMR sensor chips (NVE AA003-02E) were used during experiments for both the sensor arrays. They have an operating range from 2 – 14 Oe, saturating at 20 Oe and are only sensitive in one direction. An Arduino Duo was used to interface the array to the computer. The Java based program Processing was used to write the GUI, algorithm and calibration code.

There were two array geometries tested in this paper, each 25x25mm^2. The 5-sensor geometry (5S) used a staggered setup, while the 9-sensor geometry (9S) used a rectangular arrangement. Each sensor had 2 output pins, requiring the use of an 8:1 analog multiplexer to multiplex the signals. PCBs were designed and printed in double layer configuration.

As ferrofluid is a paramagnetic material, it should be subjected to a magnetic field to be magnetized. To generate a uniform magnetic field, various Halbach cylinders were designed using 10×10×10 mm^3 N42 magnets. Preliminary tests were conducted to ensure optimization of the design. Halbach cylinder designs were tested using Finite Element Analysis and cross referenced with actual data. Several Halbach cylinders were tested, with a summary provided in Table 1.

Table 1. Comparison of simulated and experimental results for various Halbach cylinder configurations.

Cylinder Radius	No. Magnets	Actual Field Strength (Oe)	Simulated Field Strength (Oe)	Error (%)
8 cm	16	4500	4590	2.0
5 cm	16	1810	1860	2.8
3.3 cm	12	450	466	3.5
1.75 cm	8	46	47	2.2

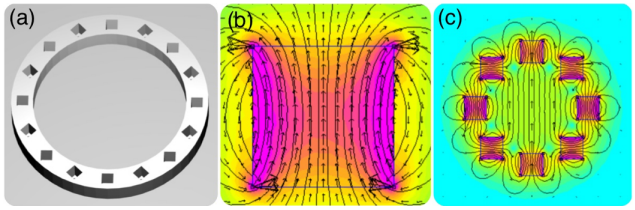

Fig. 3. (a) A rendering of a 16 magnet Halbach cylinder casing for 3D printing. (b) The singularity effect at the edges and (c) resultant density plot of a simulated Halbach Cylinder.

Note that whilst singularities did form on the corners of the magnets as shown in Fig 3b, they were acceptable because the solution was being evaluated some distance away from those points. The simulations provided a basis for what size cylinder should be used, and by extrapolating the results, we can predict the field strengths at varying cylinder sizes.

Though the 1.75 cm Halbach cylinder could induce a >20Oe magnetic field in the ferrofluid as measured by a search coil, room was needed inside the Halbach cylinder to fit all the sensors. An 8 cm Halbach cylinder was chosen instead, as it could induce a 5Oe magnetic field, which is within the linear range of the sensors, and the large radius would provide ample space for the sensor array. The cylinder was placed such that the uniform magnetic field was perpendicular to the sensitive axis of the magnetic sensors.

Testing also showed field variation of up to 50% in magnitude at the circumference as compared to the center. Though the magnetic field direction is still constant, any imperfections in soldering of the sensors could result in the field not being perpendicular to the sensitive axis, causing erroneous sensing.

In such case the calibration is a solution. It is performed using cues for the user. Once complete, the user is shown a diagram of the sensor arrangement, with a white and grey dot representing where the program has localized the particle. The white dot represents localization with both a minimum and maximum calibration values (full calibration), whilst the grey dot represents localization assuming zero as the minimum value (partial calibration). Initial tests were performed using an N42 magnet to ensure that the software was working correctly. Subsequent tests were then performed using the 8cm Halbach cylinder and 1mL of ferrofluid. The ferrofluid was kept inside a pipette and moved over the array to mimic a moving particle as shown in Fig. 4.

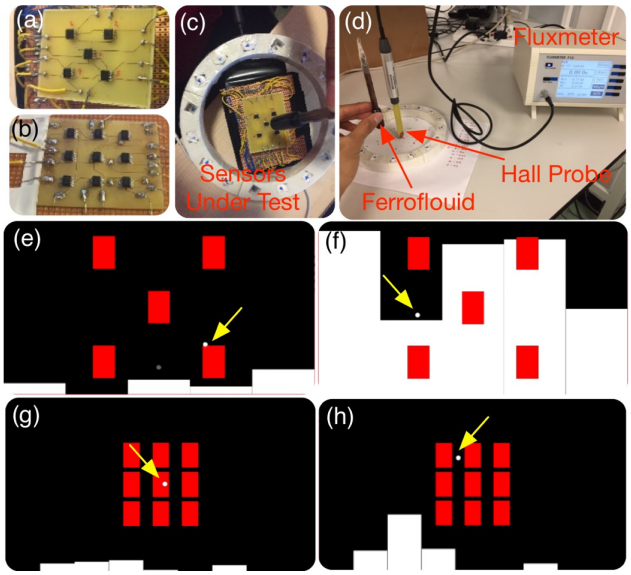

Fig. 4. (a) 5S and (b) 9S array prototypes. (c) Testing of 5S array using Halbach cylinder and ferrofluid. (d) Measurement setup for search coil experiment. Localization of ferrofluid, using both full (white dot) and partial (grey dot) calibration for (e,f) 5S and (g, h) 9S. Full calibration consistently and accurately localized the ferrofluid on the sensor array.

The results (Fig. 5) showed a stable and accurate output for the 5S array with both the magnet and ferrofluid. Compared the actual location of the magnetic source to the digital output, a mean (SD) error of 2.45 (1.61) mm and 5.45 (1.82) mm was observed for full calibration (FC) and partial calibration (PC) respectively for the ferrofluid test. This corresponds to mean error areas of 3.0% and 14.9% respectively on the 25x25mm^2 array surface. Mean (SD) errors of 1.48 (1.14) mm and 1.62 (1.26) mm were observed for FC and PC respectively for the magnet test, corresponding to mean error areas of 1.1% and 1.3%. Whilst the error for PC ferrofluid test is too high, the rest of the results show consistent and precise localization. This shows the importance of proper calibration, and also shows that the prototype and detection algorithm provide comparable results for both a strong ferromagnetic source and a paramagnetic material. Localization for the 9S sensor also provided similar results to the 5S array with the sensors, where the fully calibrated localization algorithm provided a more accurate response.

V. Conclusions

This work has successfully shown a method of localizing a paramagnetic material on a GMR sensor array in 2D. It provides a good base from which to build more complex arrays and algorithms for use in cell patterning, biosensing and tissue engineering applications. Whilst the Halbach Cylinder was an appropriate solution for a proof of concept study, an electromagnet will have to be used in the future as it will provide a more stable magnetic field with an adjustable magnitude. 3D localization algorithms should also be developed. One way this can be accomplished would be creating a simplified analytical model for the magnetic field of a magnetic dipole at the sensor values, measuring the actual

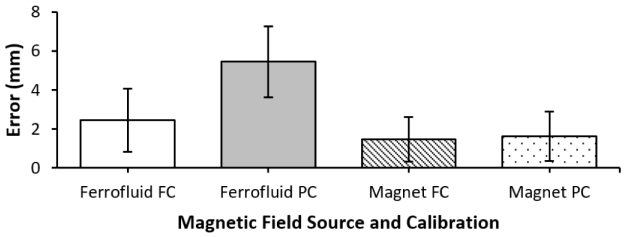

Fig. 5. Comparison of error of localization from actual position for different magnetic sources and calibrations. Ferrofluid test showing mean(SD) of 2.45(1.61) mm and 5.45(1.82) mm for FC and PC. Magnet test showing 1.48(1.14) mm and 1.62(1.26) mm.

sensor values and minimizing the error function between the two using non-linear optimization. Future applications will involve embedded sensors onto flexible analytical devices or bendable bio-compatible substrates, calling for further work into the development of a flexible magnetic sensors array and an associated localization algorithm [13,14]. Flexible arrays will also be applicable in magnetoencephalography (MEG) application to closely match various skull topologies [15].

Acknowledgment

Authors are thankful to the support received from Bendable Electronics and Sensing Technologies (BEST) group and Electronics Systems Design Centre (ESDC).

References

[1] Han, S. J., *et al.,* "CMOS integrated DNA microarray based on GMR sensors." Proc. Int. Electron Devices Meeting (IEDM), 2006.

[2] Li, S., & Wiley, I. (2011). "Biosensor nanomaterials."

[3] Graham, D. L., Ferreira, H. A., & Freitas, P. P. "Magnetoresistive-based biosensors and biochips." Trends Biotechnol, 22(9), 455-462, 2004.

[4] Rife, J. C., Miller, *et al.*,"Design and performance of GMR sensors for the detection of magnetic microbeads in biosensors." Sensors and Actuators A: Physical, 107(3), 209-218, 2003.

[5] K. M. Lei, *et al.,* "A Handheld High-Sensitivity Micro-NMR CMOS Platform With B-Field Stabilization for Multi-Type Biological/Chemical Assays," in IEEE J. Solid-State Circuits, vol. 52, no. 1, pp. 284-297, 2017.

[6] Körber, R., *et al.,* "SQUIDs in biomagnetism: a roadmap towards improved healthcare." Superconductor Science and Tech, 2016.

[7] F. Li, I. Giouroudi, and J. Kosel, "A biodetection method using magnetic particles and micro traps," J.Applied Physics, vol. 111, pp. 07B328, 2012.

[8] H. Heidari, E. Bonizzoni, U. Gatti, and F. Maloberti, "A CMOS Current-Mode Magnetic Hall Sensor With Integrated Front-End," IEEE Trans. Circuits Systems I: Regular Papers, vol. 62, pp. 1270-1278, 2015.

[9] H. Heidari, *et al.*, "A 0.18-µm CMOS Current-mode Hall Magnetic Sensor with Very Low Bias Current and High Sensitive Front-End," in Proc. IEEE SENSORS Conf., 2014, pp. 1467-1470.

[10] Birla, R. (2016). "Tissue engineering for the heart." 1st ed. Cham: Springer International Publishing, pp.31-51.

[11] Laughlin, D. E., & Hōno, K. Physical metallurgy. Volume 1, 2014

[12] Lenz, J., & Edelstein, S. "Magnetic sensors and their applications." IEEE Sensor., 6(3), 631-649, 2006.

[13] Cubells-Beltrán, M. *et al.,* "Integration of GMR Sensors with Different Technologies. Sensors", 16(6), 939, 2016..

[14] H. Heidari, *et al.*, "Towards bendable CMOS magnetic sensors," in IEEE Conf. PhD Research Microelect. Elect. (PRIME), 2015, pp. 314-317.

[15] H. Heidari, F. Liu and R. Dahiya, "Towards flexible magnetoelectronics for robotic applications," 2nd Asia-Pacific Conference on Intelligent Robot Systems (ACIRS), pp. 295-298, 2017.

[16] Körber, R., et al., "SQUIDs in biomagnetism: a roadmap towards improved healthcare." Superconductor Science and Tech, 2016.